© 2016. Published by The Company of Biologists Ltd | Journal of Cell Science (2016) 129, 3437-3448 doi:10.1242/jcs.192534

RESEARCH ARTICLE

# Bradykinin promotes neuron-generating division of neural progenitor cells through ERK activation

**Micheli M. Pillat[1], Claudiana Lameu[1], Cleber A. Trujillo[2], Talita Glaser[1], Angélica R. Cappellari[3], Priscilla D. Negraes[1,2], Ana M. O. Battastini[3], Telma T. Schwindt[1], Alysson R. Muotri[2] and Henning Ulrich[1,*]**

## ABSTRACT

During brain development, cells proliferate, migrate and differentiate in highly accurate patterns. In this context, published results indicate that bradykinin functions in neural fate determination, favoring neurogenesis and migration. However, mechanisms underlying bradykinin function are yet to be explored. Our findings indicate a previously unidentified role for bradykinin action in inducing neuron-generating division *in vitro* and *in vivo*, given that bradykinin lengthened the $G_1$-phase of the neural progenitor cells (NPC) cycle and increased *TIS21* (also known as *PC3* and *BTG2*) expression in hippocampus from newborn mice. This role, triggered by activation of the kinin-B2 receptor, was conditioned by ERK1/2 activation. Moreover, immunohistochemistry analysis of hippocampal dentate gyrus showed that the percentage of $Ki67^+$ cells markedly increased in bradykinin-treated mice, and ERK1/2 inhibition affected this neurogenic response. The progress of neurogenesis depended on sustained ERK phosphorylation and resulted in ERK1/2 translocation to the nucleus in NPCs and PC12 cells, changing expression of genes such as *Hes1* and *Ngn2* (also known as *Neurog2*). In agreement with the function of ERK in integrating signaling pathways, effects of bradykinin in stimulating neurogenesis were reversed following removal of protein kinase C (PKC)-mediated sustained phosphorylation.

**KEY WORDS: Bradykinin, ERK, Proliferation, Neurogenesis, *Ngn2*, Cell cycle**

## INTRODUCTION

During nervous system development, neural stem and progenitor cells (NPCs) perform the task of proliferating, migrating, and differentiating in highly accurate patterns. Genetic programs and specific factors in the microniches control such accuracy. These factors influence proliferative and neuron-generating cell divisions, and differentiation programs (Calegari et al., 2005; Lako et al., 2009; Lukaszewicz et al., 2002). Proliferative division is rapidly completed, given that it has an abbreviated $G_1$-phase, and generates two identical precursor cells. By contrast, neuron-generating division generates two daughter cells, where one or both leave the cell cycle and undergo differentiation. Recent *in vitro* and *in vivo* studies have demonstrated that NPCs with a longer $G_1$-phase of the cell cycle perform a neuron-generating division (Calegari et al., 2005; Calegari and Huttner, 2003; Lako et al., 2009; Lukaszewicz et al., 2002; Neganova et al., 2009; Orford and Scadden, 2008). Similarly, expression of the gene *TIS21* (also known as *PC3* and *BTG2*) at the onset of neurogenesis identifies cells switching from proliferative to neuron-generating division. Expression of this gene, in the same way as elongation of the $G_1$-phase, serves as a marker for neuron-generating division (Calegari and Huttner, 2003; Iacopetti et al., 1999).

NPCs can be obtained from the telencephalon of mice embryos, and used to reproduce *in vitro* events of cortical development *in vivo*, such as proliferation, migration, neurogenesis and gliogenesis. As observed *in vivo* (Tropepe et al., 1999), fibroblast growth factor-2 (FGF-2) and epidermal growth factor (EGF) also induce proliferative division of NPCs *in vitro*, maintaining cells as multipotent and leading to the formation of neurospheres (Lukaszewicz et al., 2002; Reynolds and Weiss, 1996). After growth factor removal and cell adhesion, NPCs differentiate spontaneously (reviewed by Trujillo et al., 2009).

Distinct dynamics of ERK1 and ERK2 (ERK1/2; also known as MAPK3 and MAPK1, respectively; hereafter referred to as ERK) activation are believed to be the underlying cause of differences in cellular responses, such as proliferation or differentiation, as described for PC12 cells treated with growth factors (Marshall, 1995; Santos et al., 2007; Sasagawa et al., 2005; Traverse et al., 1992; Vaudry et al., 2002; von Kriegsheim et al., 2009). For example, whereas EGF stimulation causes transient ERK activation in the cytoplasm and results in proliferation, nerve growth factor (NGF) induces sustained ERK activation and nuclear translocation, resulting in neuronal differentiation. To achieve the latter sustained ERK activation, several signaling pathways including those mediated by phosphoinositide 3-kinase (PI3K), Ras, $Ca^{2+}$, protein kinase C (PKC) and cAMP might be required. Once attained, sustained ERK activation followed by nuclear translocation is sufficient for induction of neurogenesis.

Recent studies have demonstrated a new role of bradykinin in promoting cell migration and neurogenesis during *in vitro* differentiation of pluripotent cells and embryonic NPCs (Martins et al., 2005; Pillat et al., 2015; Trujillo et al., 2012). The opposite occurs in NPCs treated with the kinin-B2 receptor (B2BkR, also known as BDKRB2) antagonist HOE-140 and also in NPCs from embryos of $B2BkR^{-/-}$ mice, i.e. decreased cell migration and neurogenesis. $B2BkR^{-/-}$ mice have decreased neuronal marker expression in several stages of development, suggesting the involvement of bradykinin in neuronal phenotype determination *in vivo* (Trujillo et al., 2012). However, the mechanisms triggered by bradykinin to coordinate migration, proliferation and neuronal

[1]Departamento de Bioquímica, Instituto de Química, Universidade de São Paulo, São Paulo 05508-900, Brazil. [2]Departments of Pediatrics and Cellular & Molecular Medicine, University of California San Diego, San Diego, CA 92093-0695, USA. [3]Departamento de Bioquímica, Instituto de Ciências Básicas e da Saúde, UFRGS, Porto Alegre 90035 000, Brazil.

*Author for correspondence (henning@iq.usp.br)

M.M.P., 0000-0002-6753-6083; C.A.T., 0000-0002-0675-6437; T.G., 0000-0002-3350-4569; A.R.C., 0000-0002-8202-609X; P.D.N., 0000-0001-7876-1895; T.T.S., 0000-0001-5603-7425; H.U., 0000-0002-2114-3815

**Received 3 June 2016; Accepted 27 July 2016**



Journal of Cell Science

Journal of Cell Science (2016) 129, 3437-3448 doi:10.1242/jcs.192534

differentiation remain unknown. Here, we provide mechanisms for neuron-generating divisions in NPCs and in hippocampus from newborn mice, and delineate the intracellular signaling pathways that might serve as key determinants of bradykinin-induced effects in the cell cycle followed by neuronal differentiation.

## RESULTS

### Bradykinin-mediated effects on the proliferation and cell cycle of undifferentiated NPCs – the cell cycle length predicts cell fate

EGF and FGF-2 induce proliferative division of NPCs, keeping them in their undifferentiated state (Lukaszewicz et al., 2002; Reynolds and Weiss, 1992, 1996). In this context, we evaluated the effect of bradykinin on proliferation of undifferentiated cells stimulated by growth factors. EGF and FGF-2 (both at 20 ng/ml final concentrations) were added to the culture medium 1 h prior to bradykinin (1 µM) treatment and cells were analyzed after 24 h in this medium (Fig. 1A,B). The presence of bradykinin resulted in a significant reduction in proliferation in comparison with samples treated with growth factors only, as observed by their significantly lower BrdU incorporation after 2 h of treatment ($P$=0.0126). We sought to identify in which phase of the cell cycle NPCs stimulated with bradykinin in the presence of growth factors are primarily found. For this purpose, cells were double-labeled for BrdU (after 30 min of treatment) plus propidium iodide (Fig. 1C) and Ki67 plus propidium iodide (Fig. 1D). The addition of bradykinin to cells pretreated with growth factors resulted in an accumulation of cells in $G_1$-phase, compared to samples treated only with growth factors (Fig. 1E; $P$=0.0217).

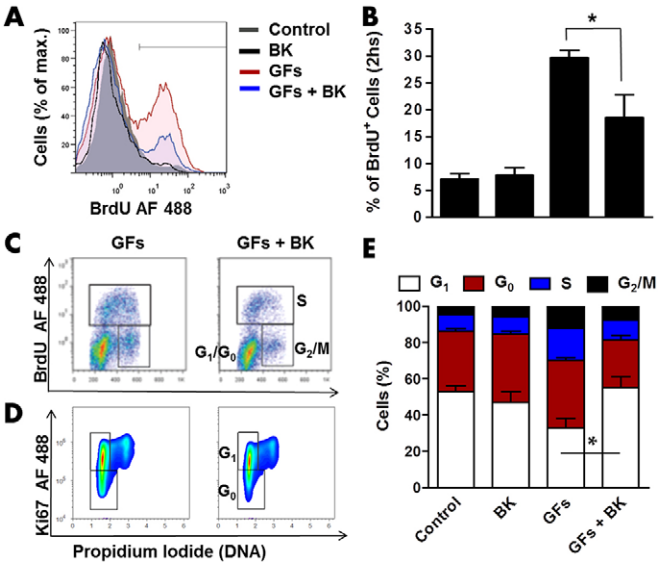


**Fig. 1. Effects of bradykinin on proliferation and cell cycle of NPCs.** (A) Growth factors (GFs; EGF plus FGF2; both at 20 ng/ml), combined or not with bradykinin (BK; 1 µM), were included in the culture medium of NPCs for 24 h, and 50 µM BrdU was added for the last 2 h of culture. Cumulative BrdU labeling was detected with Alexa Fluor (AF) 488 staining and quantified by flow cytometry. (B) Mean±s.e.m. percentages of proliferating cells ($BrdU^+$ cells) ($n$=6 independent experiments). (C) Representative dot-plots showing the number of cells in each phase of the cell cycle in NPCs treated with growth factors or growth factors and bradykinin. After a short pulse with BrdU (50 µM; 30 min), only cells in S-phase are labeled with anti-BrdU Alexa Fluor 488. (D) Representative dot-plots for Ki67 and propidium iodide fluorescence staining of undifferentiated cells treated with growth factors in the absence or presence of bradykinin. (E) Mean±s.e.m. percentage of the proportion of NPCs in each phase of the cell cycle ($n$=4 independent experiments). *$P$<0.05 (two-way ANOVA with a Bonferroni post hoc test).

It is important to stress that NPCs undergoing neuron-generating division have a longer $G_1$-phase than those performing proliferative division (which have an abbreviated $G_1$ phase) (Calegari et al., 2005; Orford and Scadden, 2008). Thus, given that the cell cycle length predicts cell fate, we assessed whether this neuron-generating ability in response to bradykinin signaling was accompanied by an increase in the length of the $G_1$-phase of the cell cycle. For this purpose two strategies were used for analysis, which are briefly described in the Materials and Methods section (Lukaszewicz et al., 2002; Nowakowski et al., 1989; Storey, 1989; Wilcock et al., 2007). Cell cycle and $G_1$-phase lengths of NPCs exposed to the growth factors EGF and FGF-2 and bradykinin were markedly increased compared to cell cycle and $G_1$-phase length of NPCs exposed to growth factors alone (Table 1), as revealed by flow cytometry experiments. These data demonstrate that proliferating NPCs in the presence of bradykinin adopted a slower cell cycle progression (longer $G_1$-phase), which is characteristic for cells that generate neurons.

### Signaling pathways activated by bradykinin in NPCs

For delineating intracellular signaling pathways that might serve as key determinants of bradykinin-induced effects in cell cycle followed by neuronal differentiation in NPCs, we examined the activities of various intracellular signaling pathways. A significant increase in intracellular cAMP concentration ($[cAMP]_i$) was observed after 1 and 2 min of exposure to bradykinin with a subsequent decay to baseline (Fig. 2A; $P$=0.012). The B2BkR can also catalyze the exchange of GTP for GDP on the α subunits of $G_i$ and $G_s$ proteins (Blaukat et al., 2000; Hall et al., 1993; Hanke et al., 2006; Liebmann et al., 1996, 1990), even though it has been often described as a prototypical $G_q$-protein-coupled receptor. Thus, we assessed if the B2BkR could also be coupled to any member of the $G_s$ or $G_i$ protein family in NPCs or if the $G_q$ protein and its downstream pathway could affect bradykinin-stimulated cAMP production. Cells were treated with cholera toxin (0.5 µg/ml; 16 h) to activate all $G_s$ proteins, with the $G_q$ protein inhibitor YM254890 (10 µM; 15 min), with the PLC-β inhibitor U73122 (10 µM; 30 min), or with the $G_i$ protein inhibitor pertussis toxin (200 ng/ml; 16 h). Samples were then stimulated or not for 2 min with bradykinin (1 µM), and changes in $[cAMP]_i$ levels were determined. Pre-treatment with only pertussis toxin prevented the bradykinin-stimulated $[cAMP]_i$ increase (Fig. 2B). In this context, it is known that βγ subunits of the $G_i$ protein can activate adenylate cyclase II, IV and VII, and that βγ subunits are sensitive to pertussis toxin (Chen et al., 1995). Therefore, our data suggest that the B2BkR is also coupled to $G_i$ proteins in NPCs, and that their βγ subunits might induce activation of adenylate cyclase and cAMP production.

Previous studies have shown that bradykinin induces an elevation in the concentration of intracellular free $Ca^{2+}$ ($[Ca^{2+}]_i$) by activating B2BkR in four models of neural differentiation (Appell and Barefoot, 1989; Martins et al., 2008, 2005; Nascimento et al., 2015; Trujillo et al., 2012). Thus, we aimed to find the intracellular signaling pathways that mediate the bradykinin-induced $[Ca^{2+}]_i$ increase. For this purpose, NPCs were pre-treated with YM254890, pertussis toxin, or YM254890 plus pertussis toxin. Surprisingly, treatments with YM254890 or pertussis toxin only partially inhibited the response of NPCs to bradykinin from 5.27±0.49 to 3.28±0.39 (37.7% of suppression) or 3.73±0.12 (29.2% of suppression), respectively (mean±s.e.m.; Fig. 2C,D). By contrast, simultaneous inhibition of both $G_q$ and $G_i$ proteins (YM254890 plus pertussis

Journal of Cell Science (2016) 129, 3437-3448 doi:10.1242/jcs.192534

**Table 1. Cell cycle distributions of NPCs treated with growth factors, and growth factors plus bradykinin**

| | | Cell cycle length (h) | | | | | |
|---|---|---|---|---|---|---|---|
| | Analysis | Complete cycle | S-phase | $G_1$+ $G_2$/M phase | $G_2$/M phase | $G_1$ phase | Proliferation fraction (%) |
| Growth factors | A | 11.41±0.72 | 2.50±0.24 | 8.9±0.62 | 2.16±0.42 | 6.74±0.62 | 73.95±5.16 |
| | B | 10.08±0.81 | 2.96±0.32 | – | 2.16±0.52 | 4.96±0.81 | – |
| Growth factors+ bradykinin | A | 17.30±0.95* | 2.40±0.37 | 14.9±0.84 | 2.20±0.31 | 12.70±0.79* | 75.50±8.75 |
| | B | 18.00±1.21* | 3.20±0.53 | – | 2.16±0.22 | 12.64±0.88* | – |

The length of each stage of the cell cycle times in hours are derived from cumulative BrdU labeling experiments and two different analysis methods, denoted A and B, as described in the Materials and Methods section. Growth factors (EGF plus FGF2; both at 20 ng/ml), combined or not with bradykinin (1 µM), were added to the culture medium of NPCs for 24 h, and 50 µM BrdU was added for the last 30 min or 2 h of culture ($n$=4 independent experiments). Data from flow cytometry are shown as mean±s.e.m. percentages for the whole population. *$P$<0.05 (two-way ANOVA with a Bonferroni post hoc test).

toxin) blocked the bradykinin-induced $[Ca^{2+}]_i$ increase (0.33±0.19; 93.7% of suppression), suggesting that both types of G proteins are involved in B2BkR-mediated responses, and that co-activation of $G_q$ and $G_i$ proteins exerts synergistic effects on bradykinin-induced $[Ca^{2+}]_i$ increases ($P$=0.0005), such as observed in experiments conducted with platelets (Shah et al., 1999). Subsequently, we provided evidence that the bradykinin-induced $[Ca^{2+}]_i$ increase occurs by mobilization of intracellular $Ca^{2+}$ stores. Pre-treatment of NPCs for 1 h with thapsigargin, an inhibitor of the sarco- and endoplasmic reticulum $Ca^{2+}$ ATPase (SERCA), completely blocked bradykinin-induced $[Ca^{2+}]_i$ increases (Fig. 2C,D; $P$=0.0002).

To determine which other signaling pathways might serve as key determinant of bradykinin effects in neural differentiation of NPCs, intracellular signal-transducing kinase activities were examined. For this, cells initially starved for 6 h were stimulated or not for 10 min with bradykinin (1 µM), followed by detection of phosphorylated (p)-STAT3, JNK family proteins (p-JNK), Akt family proteins (p-Akt) and p38 MAPK family proteins (p-p38) by flow cytometry (Fig. 2E,F). Bradykinin-treated samples did not show any significant differences in levels of phosphorylated JNK and STAT3, compared to untreated samples. In contrast, higher levels of p-p38 ($P$=0.0446) and p-Akt ($P$=0.0071) were observed after

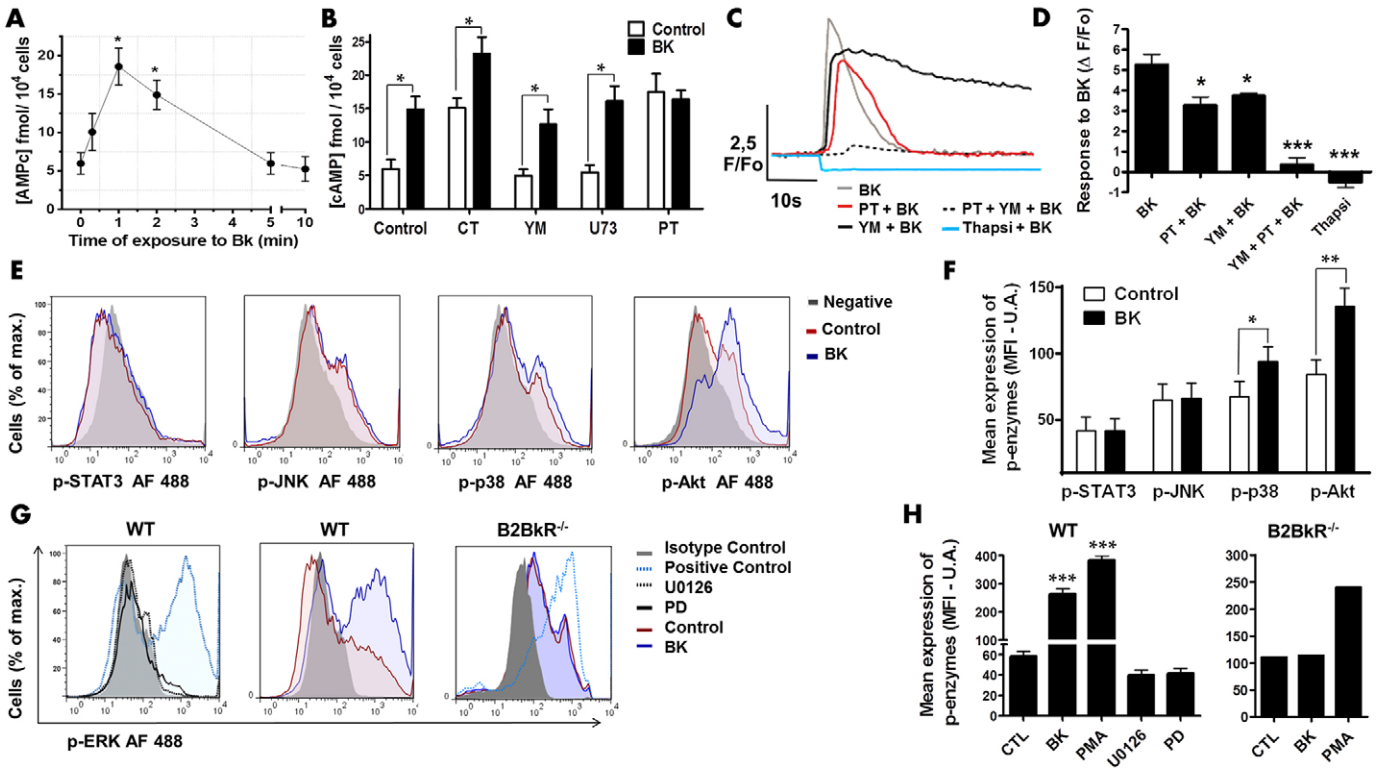


**Fig. 2. Bradykinin-induced changes in $[cAMP]_i$, $[Ca^{2+}]_i$ and phosphorylation cascades in NPCs.** (A) Kinetics of cAMP formation following stimulation with bradykinin (BK, 1 µM; $n$=4). (B) Pre-incubation with cholera toxin (CT; 0.5 µg/ml), YM254890 (YM; 10 µM), U73122 (U73; 10 µM), pertussis toxin (PT; 200 ng/ml) before bradykinin (1 µM) stimulus and $[cAMP]_i$ determination (mean±s.e.m.; $n$=4). (C) Effects of pre-treatments with pertussis toxin, YM254890 and thapsigargin (Thapsi; 1 µM) on bradykinin-induced $[Ca^{2+}]_i$ transient elevation in undifferentiated neurospheres. (D) Mean±s.e.m. values of $\Delta[Ca^{2+}]_i$ ($n$=4). (E) Representative flow cytometry histograms show staining with antibodies against the indicated phosphorylated enzyme conjugated to Alexa Fluor (AF) 488 in 6-h-starved NPCs stimulated with bradykinin (10 min). (F) Mean±s.e.m. expression levels of these phosphorylated enzymes were estimated by determining the mean fluorescence intensity (MFI) for each sample ($n$=6). (G) Wild-type (WT; $n$=6) and B2BkR$^{-/-}$ NPCs ($n$=1) were stimulated with bradykinin in the absence or presence of the U0126 (10 µM), PD98059 (PD; 20 µM) or PMA (50 ng/ml). NPCs were then stained with anti-p-ERK antibodies (AF 488) and analyzed by flow cytometry. (H) Data shown as mean±s.e.m. of p-ERK expression levels estimated by MFI. CTL, control. *$P$<0.05, **$P$<0.01, *** $P$<0.001 (Student's $t$-test and two-way ANOVA with a Bonferroni post hoc test).

Journal of Cell Science (2016) 129, 3437-3448 doi:10.1242/jcs.192534

bradykinin stimulation. It is known that several signaling pathways, such as the PI3K–Akt, PKC, $Ca^{2+}$, p38 MAPK and cAMP, can regulate ERK activation or integrate their signals in this signaling cascade (Blaukat et al., 2000; Bouschet et al., 2003; Murray, 1998; Westermarck et al., 2001). Based on this fact and known effects of ERK in controlling processes such as proliferation and neuronal differentiation, the influence of bradykinin on this MAPK was further studied (Fig. 2G,H). Phorbol 12-myristate 13-acetate (PMA) and inhibitors of MEK–ERK pathway U0126 and PD98059 were used as positive and negative controls, respectively, for ERK phosphorylation. Bradykinin increased the level of p-ERK expression when compared to control samples in neurospheres from wild-type (WT) mice ($P$=0.0001). PMA induced ERK phosphorylation, whereas bradykinin did not provoke any effect on ERK phosphorylation in neurospheres from B2BkR-knockout mice, confirming that bradykinin exerts its effects specifically through B2BkR stimulation.

The activation and regulation of ERK by one or more pathways result in distinct kinetics and cell localization, which in turn cause different cell responses. Namely, in PC12 cells, ERK induces either proliferation when activated transiently, or induces neuronal differentiation and suppression of proliferation when it remains activated for a prolonged time and translocates to the nucleus (Impey et al., 1999; Marshall, 1995; Santos et al., 2007; Sasagawa et al., 2005; Traverse et al., 1992; von Kriegsheim et al., 2009). In order to assess how long ERK activity is sustained, untreated NPCs (control) and NPCs treated with bradykinin (1 µM) for 2, 5, 10, 15, 30 and 60 min were analyzed by flow cytometry using an anti-p-ERK antibody. Bradykinin activated ERK for at least 60 min (Fig. 3A,B). NPCs starved for 6 h were kept for 15 min in the absence or presence of bradykinin (1 µM), fixed, and stained for p-ERK and the cytoplasmatic protein nestin. As observed in the representative images and bar plots (Fig. 3C,D), the proportion of cells expressing detectable levels of p-ERK in the nucleus increased significantly in bradykinin-treated samples compared to controls ($P$=0.0187). In agreement with results obtained in NPCs, bradykinin treatment induced a sustained ERK activation in PC12 cells, as revealed by flow cytometry experiments (Fig. 3A,B). Sublocalizations of ERK after bradykinin stimulation in PC12 cells starved for 6 h were further studied by using a protocol to separate nuclear and cytoplasmic protein extracts followed by western blotting assays. Increased p-ERK amounts in the nuclear extract fraction after bradykinin stimulation were observed, when compared to untreated cells (Fig. 3E,F; $P$=0.0336). No significant differences were observed in the ratio between p-ERK and total ERK concentrations in the cytoplasmic extract. NGF stimulation (positive control), as expected, resulted in an increase of p-ERK levels in the nucleus. In Fig. 3E, controls of separation efficiency confirmed the nuclear and cytoplasmic localization of histone H1 and β-actin protein, respectively.

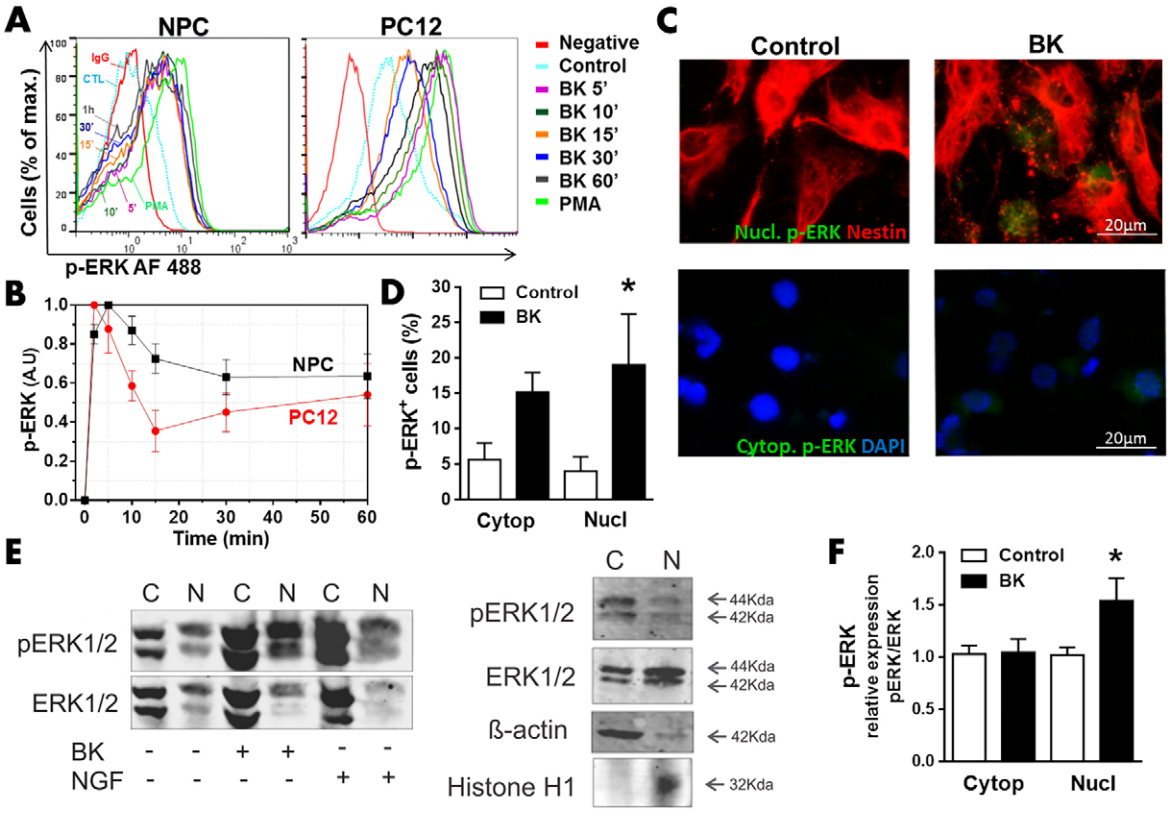


**Fig. 3. ERK phosphorylation profiles upon bradykinin (BK) stimulation of NPCs and PC12 cells.** (A) Kinetics of ERK phosphorylation (p-ERK) upon treatment of NPCs and PC12 cells with bradykinin (BK, 1 µM). Cells were unstimulated cells or stimulated with bradykinin for 5, 10, 15, 30 and 60 min or for 10 min with PMA (50 ng/ml). (B) Kinetics of p-ERK activation (mean±s.e.m. from mean fluorescence intensity, MFI) after bradykinin addition ($n$=5). (C) Nuclear or cytoplasmic distribution of p-ERK in NPCs stimulated for 15 min with bradykinin (viewed at a 200× magnification). (D) Bradykinin augmented the proportion of cells expressing detectable levels of p-ERK in the nucleus, but did not alter levels of this enzyme in the cytoplasm (mean±s.e.m., $n$=4). (E) PC12 cells were stimulated or not with bradykinin for 15 min and nuclear (N) and cytosolic (C) fractions were blotted with anti-p-ERK, anti-ERK, anti-β-actin and anti-histone H1 antibodies. Control reactions with β-actin and histone H1 immunodetection show the efficiency of cytosolic and nuclear preparations, respectively. (F) Bradykinin treatment augmented the presence of p-ERK in the nucleus (mean±s.e.m., $n$=6). *$P$<0.05 (two-way ANOVA with a Bonferroni post hoc test).

Journal of Cell Science (2016) 129, 3437-3448 doi:10.1242/jcs.192534

### Signaling pathways activated by bradykinin that modulate migration and proliferation of NPCs

As already published in earlier studies of our group, bradykinin treatment favors neural migration after differentiation of mouse and rat NPCs (Pillat et al., 2015; Trujillo et al., 2012). Neural cells present a radial migration pattern from the edge of neurospheres and the region limited by dotted lines comprised ∼95% of migrating cells. Here, we evaluated the dose–response curve of bradykinin (1 nM, 10 nM, 0.1 µM, 1 µM and 10 µM), and the involvement of PI3K–Akt, ERK and p38 MAPK pathways in bradykinin-induced neural migration. None of the pharmacological inhibitors of ERK (PD98059 20 µM; 10 µM U0126), p38 (10 µM SB203580) and PI3K–Akt (20 µM Ly294002) had any effect on cell viability (Fig. S1) and Akt activation by bradykinin occurred through PI3K, but ERK activation did not involve PI3K stimulation (Fig. S1). Although a dose of 0.1 µM of bradykinin promoted migration, because 1 µM had the maximum effect on neural migration, we used this concentration in the subsequent assay (Fig. 4A; Fig. S2). Pre-treatments with PD98059, U0126 and Ly294002 did not prevent the increase in bradykinin-induced migration. Nevertheless, inhibition of p38 MAPK by SB203580 resulted in a substantially lower number of migrating cells, and bradykinin had no effect on migration when p38 MAPK was inhibited. Cells were also treated with SB203580 plus EGF (20 ng/ml) as a positive control of the experiment. Taken together, these data suggest that bradykinin-induced cell migration during differentiation depends on p38 MAPK activation, but does not depend on the ERK and PI3K–Akt pathways.

Signaling pathways triggered by bradykinin that involved suppression of proliferative division stimulated by growth factors (FGF2 plus EGF) were investigated, by using the strategy of Dixon et al. (2002). Briefly, neurospheres were pre-treated for 30 min with EGF and FGF2 (20 ng/ml each) and then treated for 30 min with ERK (PD98059 and U0126), p38 (SB203580) and PI3K (Ly294002) inhibitors. Finally, bradykinin (1 µM) was maintained for 24 h in the culture medium. The pharmacological inhibition of ERK and p38 routes completely blocked the effect of bradykinin on suppressing growth-factor-stimulated proliferation, as shown with propidum iodide staining and quantified by flow cytometry (Fig. 4B). These results suggest that bradykinin suppressed the proliferative division of NPCs through activation of MAPKs (ERK and p38) cascades, but did not depend on the PI3K–Akt pathway ($P$=0.0487).

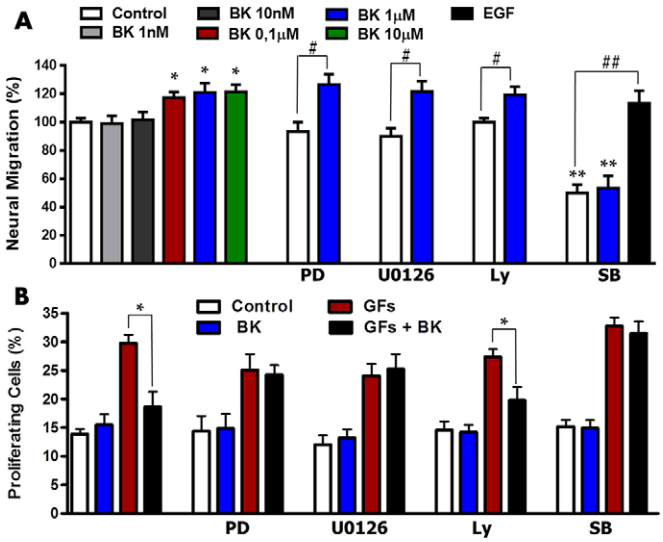


**Fig. 4. Effects of bradykinin-induced signaling on migration and growth-factor-stimulated proliferative division.** (A) Migration after 7 days of neural differentiation in the absence or presence of bradykinin (BK; 1 nM, 10 nM, 0.1 µM, 1 µM or 10 µM), U0126 (10 µM) and PD98059 (20 µM), SB203580 (10 µM), Ly294002 (30 µM) or EGF (20 ng/ml). Cells were treated with the inhibitors 1 h before bradykinin (1 µM) addition. Neural migration from the edge of neurospheres is calculated as the mean±s.e.m. percentage of basal migration. *$P$<0.05, **$P$<0.01, $^{\#}P$<0.05 versus control inhibitor, $^{\#\#}P$<0.01 versus control inhibitor (two-way ANOVA with a Bonferroni post hoc test). (B) NPC proliferation was assessed by flow cytometry analysis of propidium iodide staining. GFs, growth factors (20 ng/ml EGF, 20 ng/ml FGF2). Values are expressed as mean±s.e.m. of proliferating cells (cells in S+$G_2$/M-phase), $n$=5. *$P$<0.05 versus growth factors (two-way ANOVA with a Bonferroni post hoc test).

### Bradykinin-activated signaling pathways for NPC fate determination

It is known that bradykinin treatment results in an increase of β3-tubulin and a decrease of GFAP-positive cells (Martins et al., 2008; Pillat et al., 2015; Trujillo et al., 2012). Here, we determined expression levels of further neural markers using flow cytometry techniques (Fig. 5A,B) and qualitative immunofluorescence studies (Fig. 5C,D), and investigated bradykinin-activated signaling pathways that function in fostering NPC neurogenesis. Chronic treatment with 1 µM bradykinin throughout the course of differentiation decreased the frequency of S100β-positive cells (a glial-cell-specific protein, in agreement with a previous work of our group, Trujillo et al., 2012), whereas the frequency of MAP2-positive cells (neuron-specific protein) was significantly increased (Fig. 5A,B). These effects were confirmed by microscopic analysis of immunostained cells (Fig. 5C,D). Now, we show, by flow cytometry analysis, that bradykinin completely lost its effect to promote neurogenesis when ERK signaling was blocked by the presence of 20 µM PD98059 or 10 µM U0126 (Fig. 5E). Furthermore, under these conditions gliogenesis was promoted and neurogenesis reduced compared to the untreated control differentiation (Fig. 5E), such as observed in experiments conducted in the presence of B2BkR antagonists (Trujillo et al., 2012). The importance of ERK in the mechanisms of neurogenesis imposed by bradykinin was confirmed by microscopic analysis of immunostained cells (Fig. 5F,G).

In this context, it is well known that Hes1 is a repressor-type basic helix-loop-helix (bHLH) gene in neurogenesis, given that it inhibits neurogenic bHLH transcription factors, such as MASH1 (also known as Ascl1) and Ngn2 (neurogenin 2, also known as Neurog2) (Kageyama et al., 2008). Thus, it is important to stress that Hes1 inactivation leads to acceleration of neurogenesis (Imayoshi et al., 2008). Expression of *Hes1* mRNA was downregulated in NPCs in response to bradykinin stimulation (Fig. 5I). Interestingly, we found that bradykinin completely lost its effect on *Hes1* expression under conditions of ERK inhibition. Moreover, expression of the neurogenic factor *Ngn2* was significantly upregulated in response to bradykinin treatment, whereas pre-treatment with U0126 prevented this bradykinin-promoted effect (Fig. 5I). Taken together, these results confirm the importance of ERK in the mechanisms of neurogenesis imposed by bradykinin.

A further question was whether bradykinin exerts its effects in modulating differentiation through the PI3K–Akt or p38 MAPK pathways. Immunofluorescence and flow cytometry data shown in Fig. 5E and H, respectively, revealed that, even when PI3K–Akt is inhibited, bradykinin induced an increase in the percentage of cells expressing β3-tubulin and a decrease in the percentage of cells

Journal of Cell Science (2016) 129, 3437-3448 doi:10.1242/jcs.192534

expressing GFAP at the end of differentiation (day 7). These data suggest that bradykinin acts on NPC differentiation independently from the PI3K–Akt pathway. Inhibition of p38 MAPK in the presence of bradykinin increased the population of cells expressing β3-tubulin and reduced the percentage expressing GFAP in comparison to control experiments (Fig. 5E,H). Thus, SB203580 plus bradykinin treatment resulted in similar effects to those observed in bradykinin-treated samples during differentiation. These data suggest that bradykinin acts in modulating NPC differentiation independently from the p38 pathway.

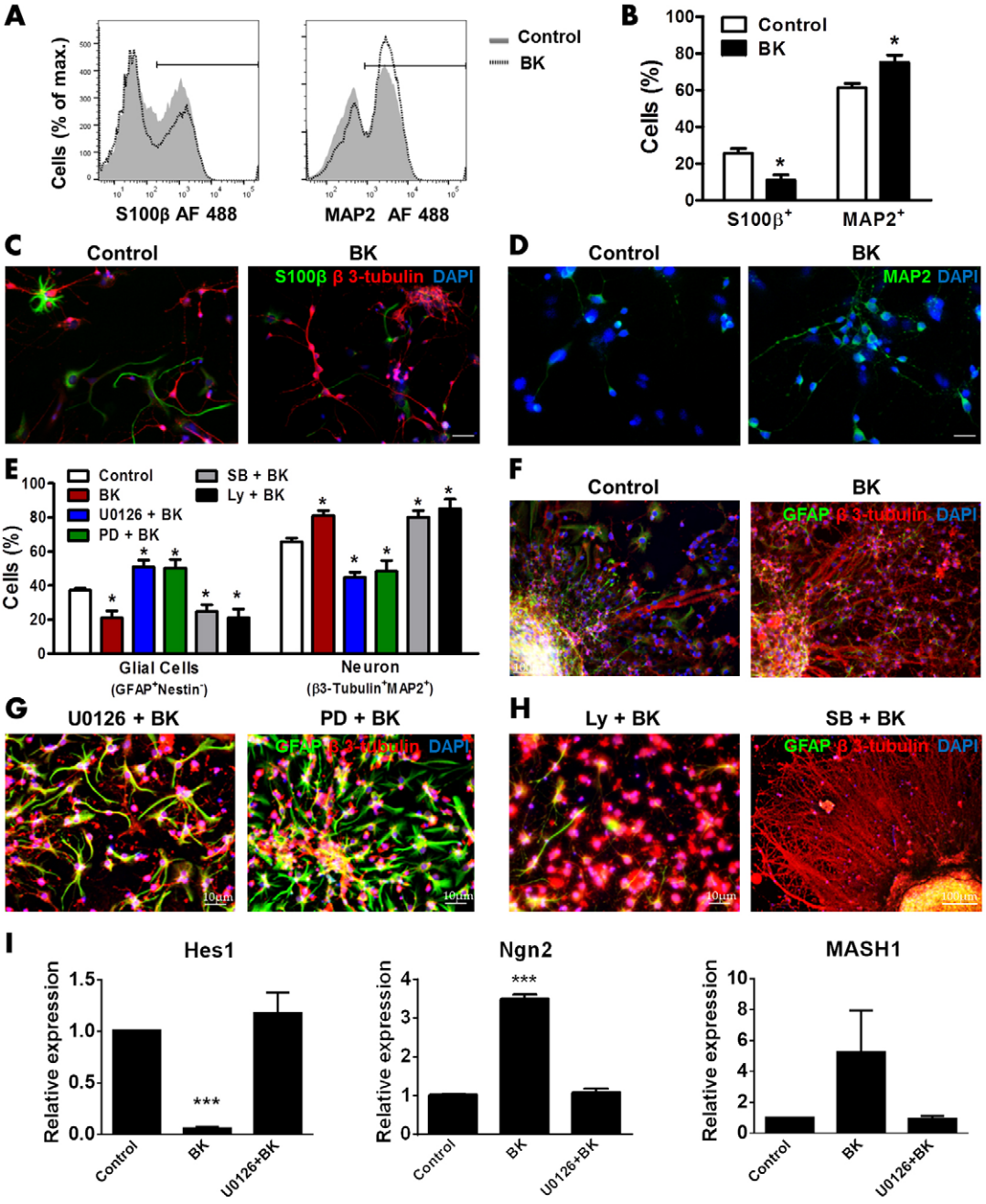


**Fig. 5. Effects of bradykinin-induced signaling on differentiation of mouse NPCs.** (A) Representative flow cytometry histograms comparing frequencies of cells expressing S100β and MAP2 in mouse NPCs differentiated for 7 days in the absence (control; solid gray histogram) or presence of 1 µM bradykinin (BK, black dotted line). Both secondary antibodies were conjugated to Alexa Fluor (AF) 488. (B) Mean±s.e.m. of percentage of S100β$^+$ (in agreement with a previous work of our group, Trujillo et al., 2012) and MAP2$^+$ cells. Qualitative immunostaining shows differences in S100β$^+$ (green) and β3-tubulin$^+$ (red) cells (C) or MAP2$^+$ (green) cells (D) between control and 1 µM bradykinin-treated neurospheres during differentiation. DAPI-labeled nuclei were used for cell counting. (E) Neurospheres were differentiated in the presence or absence of U0126 (10 µM), PD98059 (PD, 20 µM), Ly294002 (Ly, 20 µM) or SB203580 (SB; 10 µM). Cells were treated with the inhibitors 1 h before bradykinin (1 µM) addition. Flow cytometry data for GFAP (AF 488) versus nestin (AF 555), and MAP2 (AF 488) versus β3-tubulin (AF 555) expression in differentiated neurospheres were obtained in the absence or presence of treatments described above. Data are presented as mean±s.e.m. percentages of glial cells (GFAP$^+$ nestin$^-$) or neurons (MAP2$^+$ β3-tubulin$^+$). (F,G,H) Neurospheres were treated, fixed and stained with anti-β3-tubulin (AF 555; red) and anti-GFAP (AF 488; green) antibodies. (I) *Hes1*, *Ngn2* and *MASH1* gene expression levels in the absence or presence of bradykinin and/or U0126. Data are representatives of at least three independent experiments and shown as mean±s.e.m. *$P$<0.05, ***$P$<0.001 (Student's *t*-test and two-way ANOVA with a Bonferroni post hoc test). Scale bars: 10 µm.

Journal of Cell Science (2016) 129, 3437-3448 doi:10.1242/jcs.192534

### Rewiring ERK dynamics redirects phenotypic response to bradykinin

Given that in molecular mechanistic investigations of neurogenesis, PC12 cells provide a broad basis for comparison with previous studies, we also made use of this model in this study. We initially investigated the differentiation of non-treated (control, CTL), NGF-treated (50 ng/ml) or bradykinin-treated (1 µM) PC12 cells on an adherent matrix of poly-L-lysine and laminin for 48 h. NGF induced differentiation as expected, and bradykinin also enhanced differentiation because we observed a significant increase in the number of cells with more than three neurites ($P$=0.0334) and a reduction in the percentage of cells without neurites ($P$=0.0280) (Fig. 6A,B). As already mentioned, transient and sustained ERK activation regulates cell fates, such as growth and differentiation, in PC12 cells (Marshall, 1995; Santos et al., 2007; Traverse et al., 1992; Vaudry et al., 2002). Here, we performed the same kinetic experiments of ERK stimulation by EGF and NGF, which induce transient and sustained ERK activation, respectively (Fig. 6C,D). Additionally, it has been demonstrated that sustained ERK activation occurs by stimulation of two or more pathways that integrate activating this MAPK. Thus, the initial transient and the subsequent sustained phase can be disrupted (York et al., 1998). In view of that, we modulated the kinetics of ERK activation by bradykinin in order to evaluate the importance of sustained ERK activation in neurogenesis induction. For this, classical PKCs (cPKCs; activated by $Ca^{2+}$, diacylglycerol and phosphatidylserine)

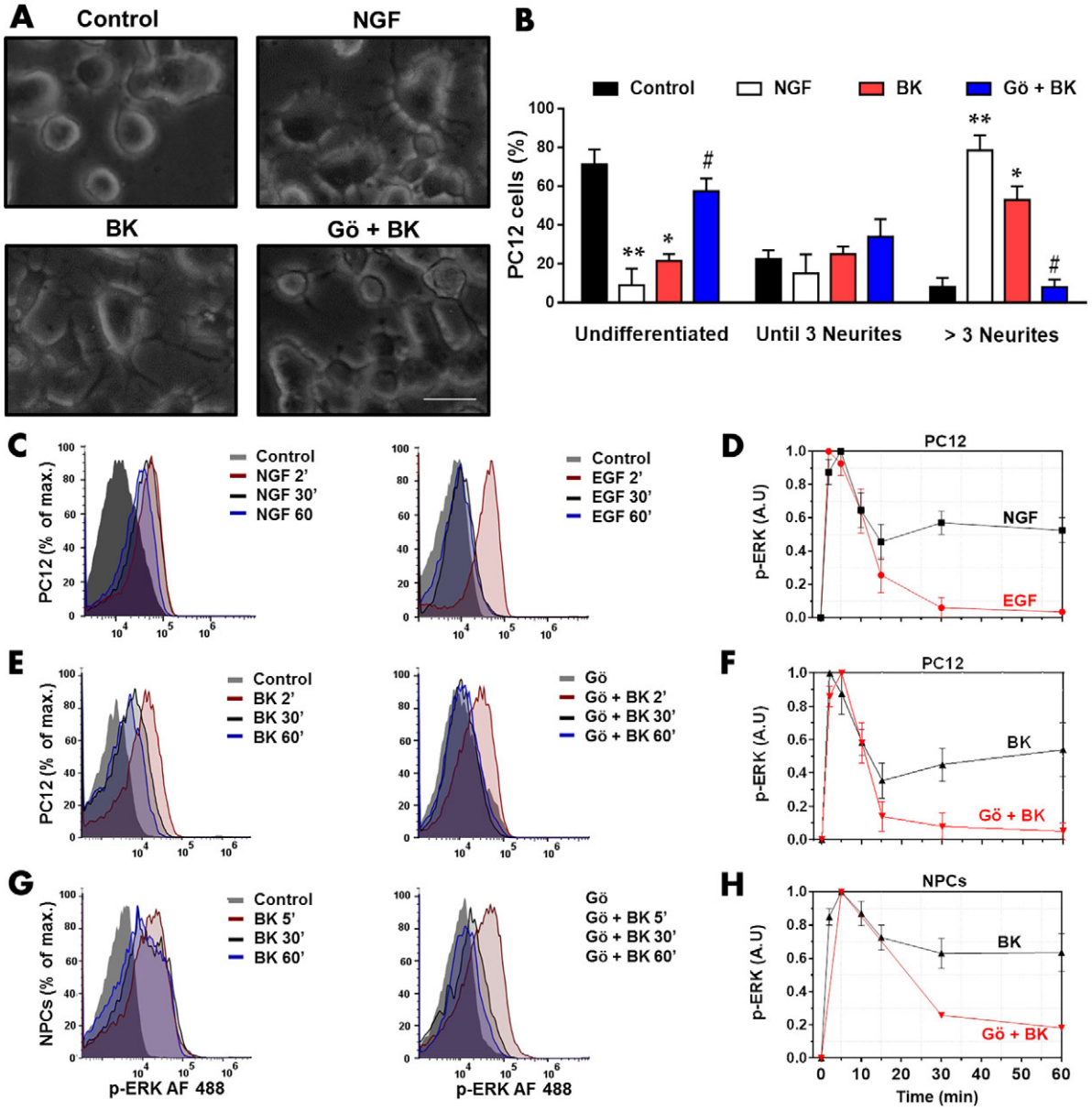


**Fig. 6. Rewiring ERK dynamics redirects phenotypic response to bradykinin.** (A) Representative images of neural differentiation of PC12 cells following NGF (50 ng/ml), bradykinin (BK, 1 µM) and Gö6973 (Gö; 10 µM) treatment for 48 h captured by differential interference contrast (DIC) microscopy. Scale bar: 10 µm. (B) Mean±s.e.m. percentages of undifferentiated (without neurites) or differentiated cells (with three or more neurites) after indicated treatment. Histograms and quantification of time-dependent ERK activity profiles upon stimulation with NGF or EGF (C,D), BK and Gö+BK (E,F) in PC12 cells, and BK and Gö+BK in NPCs (G,H), obtained by flow cytometry analysis. Data are shown as mean±s.e.m. of p-ERK-immunostaining ($n$=4). *$P$<0.05, **$P$<0.01 versus control, $^{\#}P$<0.05 versus bradykinin (two-way ANOVA with a Bonferroni post hoc test).

Journal of Cell Science (2016) 129, 3437-3448 doi:10.1242/jcs.192534

were inactivated by using the inhibitor Gö6973 (Gö; 10 µM; 1 h). Fig. 6E,F shows that pre-treatment with Gö blocked sustained ERK activation stimulated by bradykinin. In other words, bradykinin started to activate ERK only transiently, similar to effects of EGF stimulation. Additionally, pre-treatment with Gö (Fig. 6G,H) and thapsigargin (1 µM for1 h; Fig. S1F,G) significantly decreased sustained ERK activation stimulated by bradykinin in NPCs. We can conclude, in advance, that ERK is activated by the integration of two or more pathways (including $Ca^{2+}$ and cPKCs) upon stimulation with bradykinin in NPCs and PC12 cells. Thus, it is possible that the activation of ERK, regardless of $Ca^{2+}$ and/or cPKC, comes from the cAMP (Bouschet et al., 2003) and/or Ras (Blaukat et al., 2000) and/or β-arrestin pathway (Khoury et al., 2014). In this context, it is known that some these pathways synergistically activate ERK. Moreover, each of them is individually necessary for attaining the profile of sustained ERK activation in PC12 cells (Bouschet et al., 2003; von Kriegsheim et al., 2009). Therefore, given that cPKC was necessary to attain the sustained ERK activation, i.e. the pre-treatment with Gö removed sustained ERK activation by bradykinin, we evaluated its effect on neuronal differentiation. The pre-treatment with this inhibitor reversed the bradykinin effect on neuritogenesis (Fig. 6A,B; cells with more than three neurites, $P$=0.0396, versus bradykinin and cells without neurites, $P$=0.0306 versus bradykinin), suggesting that sustained ERK activation might be a mechanism of inducing neurogenesis by bradykinin.

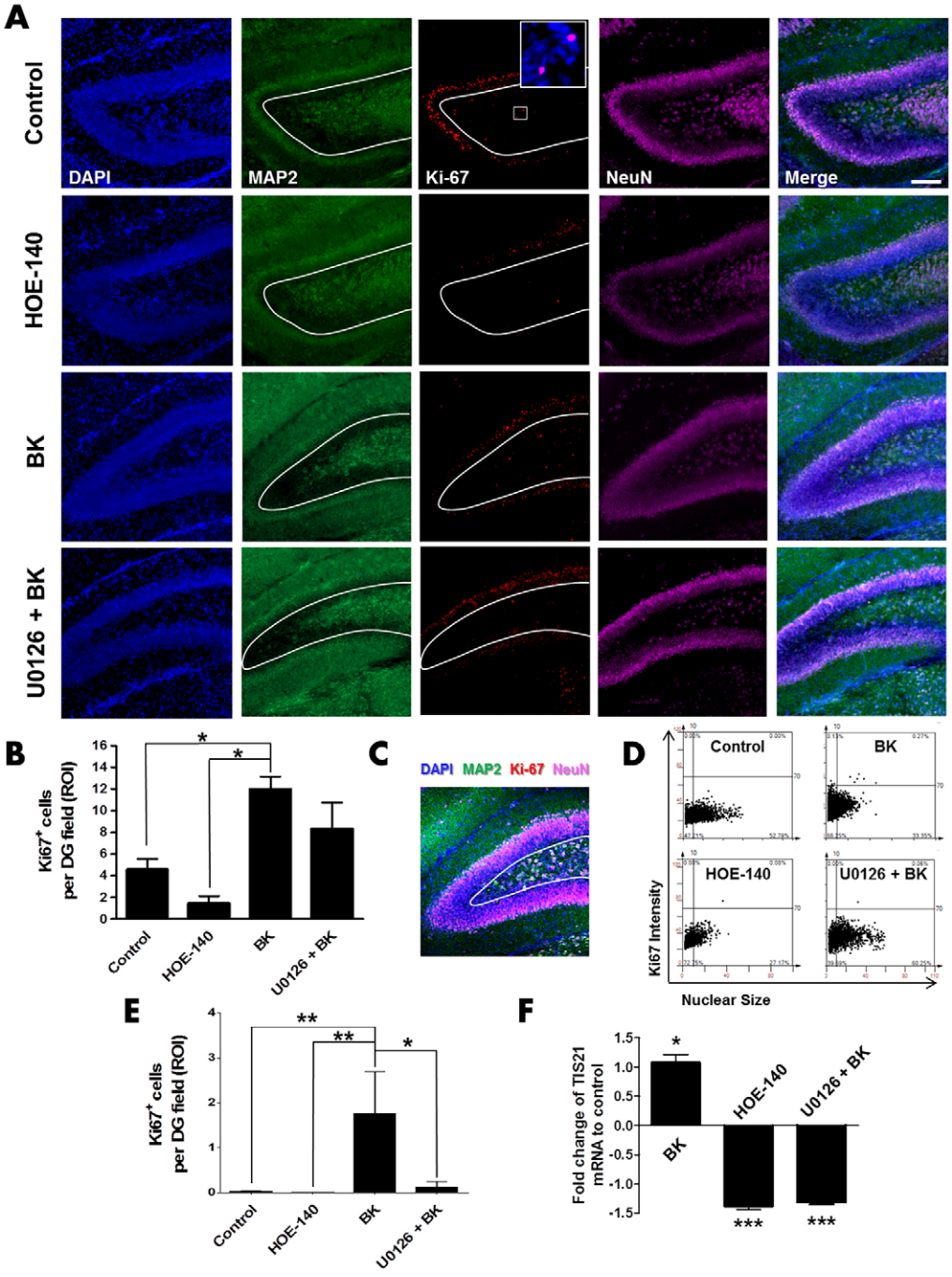


**Fig. 7. Effect of bradykinin on neurogenesis *in vivo*.** The ventricles of newborn mice (P0–P1) were injected with vehicle, bradykinin (BK, 1 µM), HOE-140 (1 µM) or U0126 (10 µM). After 1 week, P7–P8 mice were deeply anesthetized and the brains were dissected carefully. (A) Sections were triply labeled for MAP2 (green) and Ki67 (red) and NeuN (lilac) immunofluorescences. Scale bar: 100 µm. (B) Quantification of $Ki67^+$ cells in the neurogenic zone of the hippocampal dentate gyrus (white lines in A show ROIs). The number of animals was four in each group. Data are shown as mean±s.e.m. (C) Representative merged channels showing a ROI analyzed by tissue cytometry using the StrataQuest™ software. (D) Quantitative *in situ* analysis of Ki-$67^+$ nuclei in the neurogenic zone by tissue cytometry. DAPI was used as master channel to identify all nuclei in the ROI. For each nucleus the DAPI area (i.e. nuclear size, *x*-axis) and the relative fluorescence intensity as the '70% percentile' (i.e. the mean intensity of the 30% of brightest pixels in the Ki67 channel per nucleus) were measured. The cut-off for the *x*-axis was set to 10 µm in order to distinguish between prominent nuclei as well as small nuclei and potential segmentation artifacts. The cut-off for the *y*-axis was set to 70 as only strong red signals were accepted as clearly $Ki67^+$. Thus, the number of $Ki67^+$ cells in the neurogenic zone of each sample appears in the upper right quadrant of each dot plot. (E) Quantification of $Ki67^+$ cells in ROI with the StrataQuest software. Data are shown as mean±s.e.m. (F) Quantification by real-time PCR of *TIS21* mRNA expression (fold change compared to control) in cell lysates from hippocampus after 24 h of treatment with bradykinin, HOE-140 or U0126 and bradykinin ($n$=4 animals in each group, the experiments were conducted in triplicate). *$P$<0.05, ***$P$<0.001 (two-way ANOVA with a Bonferroni post hoc test).



Journal of Cell Science

Journal of Cell Science (2016) 129, 3437-3448 doi:10.1242/jcs.192534

### Influence of the bradykinin signaling on hippocampal neurogenesis

Finally, we investigated whether bradykinin and the ERK pathway affect cell division and neurogenesis *in vivo*. To assess this question, we injected (1 µl) vehicle, bradykinin (1 µM), HOE-140 (1 µM) or U0126 (10 µM) into the ventricles of newborn mice [postnatal day (P)0–P1]. After 1 week, mice (P7–P8) were deeply anesthetized and brains were dissected carefully. Sections were labeled for MAP2 (green), Ki67 (red), DCX (doublecortin; red), and NeuN (lilac) (Fig. 7A; Fig. S3A). It is important to stress that analysis of the proliferation rate in the neurogenic zone of the hippocampal dentate gyrus [region of interest (ROI) shown in Fig. 7A] is relevant, because this zone is composed of quiescent stem cells, and the proliferation of these cells is the first step in the process of neurogenesis (Orford and Scadden, 2008). For better characterization of the influence of bradykinin signaling on neurogenesis *in vivo*, proliferating cells ($Ki67^+$ cells) within ROIs were quantified by two methods, (1) standard immunohistochemistry analysis counting $Ki67^+$ cells (Fig. 7B) and (2) automatic analysis of these cells by StrataQuest software (Fig. 7C–E). Fig. 7C shows merged channels and ROI analyzed by this software, whereas Fig. 7D presents representative dot-plots of nuclear size versus relative fluorescence intensity of Ki67. Both types of analysis revealed that the presence of $Ki67^+$ cells in the ROI was markedly increased in bradykinin-treated mice compared with those treated with vehicle or HOE-140 (Fig. 7B,E). Furthermore, under these conditions, bradykinin significantly lost its effect when ERK signaling was blocked by the presence of 10 µM U0126, as determined by StrataQuest software analysis (Fig. 7E).

The neurogenic effect of bradykinin and the importance of ERK in the mechanisms imposed by this kinin *in vivo* were also analyzed by microscopic analysis of DCX (a neurogenic marker) expression levels in neurogenic zone of the hippocampal dentate gyrus, estimated by mean fluorescence intensity (MFI) in ROIs (Fig. S3). In fact, levels of DCX were upregulated in response to bradykinin, and pre-treatment with U0126 prevented this bradykinin effect.

Under the same conditions, we also evaluated the expression of the *TIS21* mRNA in hippocampus of P1–P2 mice by real-time PCR, given that this gene is specifically expressed in stem cells that, at their next division, will generate postmitotic neurons, but not in proliferating stem cells (Iacopetti et al., 1999). Expression of the *TIS21* mRNA in the stem cells occurs specifically during $G_1$-phase of neuron-generating divisions (Calegari and Huttner, 2003; Iacopetti et al., 1999). We observed that *TIS21* mRNA was markedly increased in bradykinin-treated mice ($P$=0.0225; Fig. 7F; 216% of control signal). Importantly, the responses of HOE-140 and U0126 plus bradykinin-treated mice were significantly lower than those of the vehicle-treated mice ($P$=0.0001 and $P$=0.0006, respectively; ∼30% of control signal). In other words, bradykinin-induced *TIS21* expression required the ERK signaling pathway. Taken together, these data demonstrate that bradykinin induces neuron-generating divisions *in vivo* and suggest that ERK is involved in effector mechanisms of neurogenesis triggered by bradykinin.

## DISCUSSION

Here, we studied the underlying mechanisms of bradykinin-induced neurogenesis. Among the main findings, we highlight the influence of bradykinin on division of undifferentiated NPCs. The change of type of cell division mediated by this kinin is dependent on ERK activity, as is shown by elongation of $G_1$-phase of NPCs cycle *in vitro* and *TIS21* expression *in vivo*, characteristics of neuron-generating division (Calegari and Huttner, 2003; Iacopetti et al., 1999; Neganova et al., 2009). Bradykinin evokes sustained ERK activation with its concomitant translocation to the nucleus in NPCs and PC12 cells. This type of dynamics of ERK activation is well known for resulting in neurogenesis of PC12 cells (Marshall, 1995; Sasagawa et al., 2005; Traverse et al., 1992; Vaudry et al., 2002). The results presented in this study, including the modulation of ERK kinetics, followed by the redirection of phenotype induced by bradykinin, suggest that the sustained ERK activation and translocation to the nucleus is the mechanism of bradykinin action in fostering neurogenesis. Moreover, ERK inhibition blocked the bradykinin effect in downregulating expression of *Hes1*, a repressor of NPC neuronal differentiation (Imayoshi et al., 2008; Kageyama et al., 2008; Nakamura et al., 2000), and blocked the effect of bradykinin in upregulating expression of *Ngn2*, a neurogenic transcription factor. Additionally, p38 MAPK is involved in the action of bradykinin in promoting migration during differentiation (a schematic representation for the proposed mechanism of bradykinin action is demonstrated in Fig. S4).

It is known that bradykinin stimulates proliferation in quiescent cells, but suppresses it in cells under intense mitogenic stimulus (Dixon et al., 2002; Duchene et al., 2002). Therefore, our findings showing that bradykinin suppresses proliferation stimulated by growth factors (FGF2 plus EGF) are in agreement with previous studies. At the same time, it is known that growth factors maintain multipotent NPCs by stimulating proliferative divisions, but these cells remain subject to the influence of microenvironment, especially during the $G_1$ phase (Lukaszewicz et al., 2002; Reynolds and Weiss, 1996). We observed that bradykinin leads to an elongation of $G_1$ phase and cell cycle. Thus, given that the prolongation of $G_1$ phase results in commitment to neuronal differentiation by substituting proliferative divisions for neuron-generating divisions (Calegari and Huttner, 2003; Lako et al., 2009; Neganova et al., 2009), bradykinin could be fostering neurogenesis by increasing $G_1$-phase duration and thus removing NPCs from the proliferative division induced by growth factors. We also observed that bradykinin leads to neuron-generating division *in vivo* because it increases expression of the *TIS21* mRNA and Ki67 staining of cells in hippocampal dentate gyrus. Thus, the apparent paradoxical results of global proliferation in the *in vitro* and *in vivo* model of bradykinin treatment can be explained because in the neurosphere model, cells are proliferating whereas in the hippocampal dentate gyrus they are in a quiescent state.

Many studies support the hypothesis that prolonged activation kinetics, together with nuclear translocation of ERK, provide specificity for this signal and constitute the dynamics of its activation, which is necessary and sufficient to result in the neurogenic response in PC12 cells and, possibly, in P19 cells (Bouschet et al., 2003; Ebisuya et al., 2005; Reffas and Schlegel, 2000; Santos et al., 2007; Sasagawa et al., 2005; Traverse et al., 1992). The present study is the first to investigate the kinetics and sublocalization of ERK after stimulation with bradykinin in undifferentiated neural cells (PC12 cells and NPCs), verifying a mechanism of sustained activation and nuclear translocation similar to that induced by neurogenic factors, such as NGF, PACAP and retinoic acid (Marshall, 1995; Reffas and Schlegel, 2000; Vaudry et al., 2002). Additionally, we investigated the involvement of ERK in the differentiation of NPCs and PC12 cells. ERK inhibition blocked the bradykinin effect in downregulating expression of transcriptional repressor *Hes1* and upregulating expression of neurogenic transcription factor *Ngn2*. Moreover, we observed that

Journal of Cell Science (2016) 129, 3437-3448 doi:10.1242/jcs.192534

both the direct inhibition of the MEK–ERK pathway with U0126 and PD98059 as well as the inhibition of one of its upstream pathways (Gö6973; cPKC inhibitor), prevented neurogenesis triggered by bradykinin. The inhibition of cPKC suggests the importance of the specific dynamics of ERK activation induced by bradykinin for neurogenic processes in PC12 cells. This experimental approach disregards a possible influence of cPKC in differentiation that is independent of the ERK pathway; however, it was sufficient to propose the role of sustained ERK activation by NGF in fostering differentiation (Santos et al., 2007). Considering the effects of bradykinin on neurogenesis in NPCs and PC12 cells, the dynamics of ERK activation is suggested to be implicated in the mechanisms of bradykinin-induced neurogenesis.

## MATERIALS AND METHODS

### Culture of NPCs and PC12 cells

NPCs were isolated by dissection of embryo telencephalons (day 13.5) of wild-type and B2BkR$^{-/-}$ C57BL/6 mice (provided by University of São Paulo and Federal University of São Paulo). Mice were killed with carbon dioxide. All animal experiments were carried out according to protocols of the ethics committee (authorization number: 10/2013). Embryo telencephalons were isolated and dissociated mechanically and by enzymatic action of trypsin. $2\times10^5$ cells/ml were seeded in 2% (v/v) B-27 (Life Technologies, Carlsbad, CA), Dulbecco's modified Eagle's medium (DMEM) with Ham's F-12, 20 ng/ml EGF, 20 ng/ml FGF2 (Sigma-Aldrich, St Louis, MO) and antibiotics. Neurospheres were seeded on poly-L-lysine- and laminin-precoated plastic flasks and cultured in the presence of B-27 for differentiation (Reynolds and Weiss, 1996; Trujillo et al., 2012).

PC12 rat pheochromocytoma cells ATCC No. CRL-1721 (Tischler and Greene, 1975) were maintained in DMEM supplemented with 10% (v/v) FBS, 5% horse serum (Life Technologies), glutamine and antibiotics. For starvation conditions, cells were kept overnight in DMEM supplemented with 1% horse serum. For induction of differentiation, PC12 cells were then plated on adherent poly-L-lysine- and laminin-pre-coated cell culture grade dishes for 2 days.

Cells were treated with U0126 (10 µM; Cell Signaling Technology, Danvers, MA), PD98059 (20 µM; Sigma-Aldrich, St Louis, MO), Ly294002 (20 µM; Tocris Bioscience, Bristol, UK), SB203580 (10 µM; Cell Signaling Technology), PMA (1 µM; Tocris Bioscience), U73122 (10 µM; Sigma-Aldrich), Gö6973 (10 µM; Tocris Bioscience), YM254890 (10 µM; Astellas Pharma Ins., Miyukigaoka, Tsukuba, Japan), cholera toxin (0.5 µM; Sigma-Aldrich), pertussis toxin (200 ng/ml; Sigma-Aldrich), bradykinin (1 µM; Tocris Bioscience) and HOE-140 (1 µM; Tocris Bioscience). It is known that B2BkR sequestration is rapid (half-life of 5 min) (Lamb et al., 2001; Munoz et al., 1993), but in view of possible reappearance of accessible receptors, we added bradykinin into culture medium every day during the migration and differentiation processes.

### Intracellular cAMP and $[Ca^{2+}]_i$ measurements

NPCs were untreated or pretreated and lysed directly in culture wells. Cyclic AMP (cAMP) production was measured by the Amersham cAMP Biotrak Enzymeimmunoassay (EIA) System (GE Healthcare, Waukesha, WI) according to the manufacturer's procedures.

For measurements of changes in intracellular free $Ca^{2+}$ concentration ($[Ca^{2+}]_i$), NPCs were loaded with Fluo3-AM (5 µM) for 30 min at 37°C in DMEM-F12 plus 0.5% $Me_2SO$ and 0.06% nonionic surfactant pluronic acid F-127 (Sigma-Aldrich) (Martins et al., 2005). After 30 min of incubation with Fluo-3AM, the cells were exposed to extracellular buffer and $[Ca^{2+}]_i$ imaging was immediately performed with an inverted research microscope ECLIPSE-TiS (Nikon, Melville, NY) equipped with a 14-bit high-resolution CCD camera CoolSNAP HQ2 (Photometrics, Tucson, AZ). Fluorescence emission was recorded at 515–530 nm with image acquisition rates of one frame per second; results were further analyzed with the NIS-Element AR software (Nikon). Forty cells were analyzed for each data point and $[Ca^{2+}]_i$ levels were estimated by mean variation between Fluo-3AM fluorescence intensities obtained upon stimulation with bradykinin (F) and in the resting state ($F_0$) divided by $F_0$ ($\Delta F/F_0$).

### Injection and immunohistochemistry

Prior to making an intracranial injection of the drugs, newborn pups (P0–P3) were anesthetized by hypothermia, and mounted in stereotactic apparatus. 1 µl of the solution was injected using a 5 µl Hamilton syringe (32 gauge needle) in two injection sites, 1 mm from the midline between the Bregma and Lambda and 1–2 mm deep into the anterior lateral ventricles. The pups were then placed on a heating pad for 3–5 min and returned to their mother for further recovery. Mice (P7–P8) were deeply anesthetized with ketamine and xylazine and their brains were carefully dissected. After 48 h of incubation in 4% paraformaldehyde (PFA), brains were cryoprotected in 30% sucrose, and sectioned at a 40-µm thickness using a sledge microtome. Free-floating sections of the entire hippocampus were washed and incubated for 2 h in a blocking solution (3% FBS, 0.1% Triton X-100 in PBS). Next, sections were incubated overnight at 4°C with rabbit anti-DCX (1:500; cat. no ab18723, Abcam, Cambridge, MA), rabbit anti-Ki-67 (1:1000; cat. no ab15580, Abcam), chicken anti-MAP2 (1:2500; cat. no ab5392, Sigma-Aldrich, St-Louis, MO) and mouse anti-NeuN (1:1000; cat. no MAB377, Chemicon-Millipore, Billerica, MA) primary antibodies. After 24 h, sections were washed and incubated for 2 h at room temperature with secondary Alexa-Fluor-conjugated (1:1000; Life Technologies) antibodies. Sections were washed, incubated with DAPI and mounted with DPX. Images were obtained with a fluorescence microscope (Axiovert 200, Zeiss), and analyzed with the Zen 2 software (Oberkochen, Germany) or StrataQuest software (TissueGnostics GmbH, Vienna, Austria). Briefly, the StrataQuest software is part of the TissueFAXS™ Cytometry platform – a means of image cytometry of tissue sections, tissue- and cell-cultures with a workflow and data display similar to flow cytometry. The software provides cellular data in dot-plots to show multiple measurement parameters of single cells, multicellular structures and/or morphological features. Cut-off values based on negative controls can be set to determine positive or negative cell populations as observer-independent measurements. Gates are also available to identify or work with cellular sub-populations.

### Immunocytochemistry

Differentiated neurospheres were fixed in 4% PFA for 20 min and then incubated for 20 min in PBS plus 3% FBS and 0.1% Triton X-100. After that, cells were incubated with rabbit anti-GFAP (1:500; cat. no. Z0334, DAKO Systems), rabbit anti-p-ERK (1:200; cat. no. 4370S, Cell Signaling Technology), mouse anti-β3-tubulin (1:500; cat. no. T8660, Sigma-Aldrich), rabbit anti-S100β (1:200; cat. no. G4546, Sigma-Aldrich), rabbit anti-MAP2 (1:500; cat. no. 4542S, Cell Signaling Technology) or mouse anti-Nestin (1:500; cat. no. MAB353, Millipore, Billerica, MA) antibodies for 2 h. Sequentially, samples were washed twice and incubated at room temperature with Alexa-Fluor-488-conjugated antibodies (1:1000; Life Techologies) for 1 h. After that, cells were incubated with DAPI solution (Sigma-Aldrich, 0.3 µg/ml) and mounted with DPX. Images were obtained with a fluorescence microscope (Axiovert 200, Zeiss) (Trujillo et al., 2012).

### Flow cytometry analysis of neural marker proteins and phosphorylated proteins

Experiments for quantification of neural marker proteins were performed according to Trujillo et al. (2012). Neurospheres were dissociated from the flasks using trypsin and FBS. Single cells were washed with PBS, fixed for 20 min in ice-cold 4% PFA, washed with PBS 3% FBS, and incubated with same antibodies described above in PBS plus 0.1% Triton X-100 and 3% FBS for 30 min and, then, analyzed in a flow cytometer.

Flow cytometry experiments for measurement of phosphorylated proteins were performed as previously described (Chow et al., 2001; Krutzik and Nolan, 2003; Santos et al., 2007). Briefly, 6-h-starved NPCs were stimulated and fixed for 10 min by adding 16% PFA directly into the culture medium to obtain a final concentration of 4% of PFA. Cells were then permeabilized by adding 90% ice-cold ethanol and incubated at 4°C for a least 10 min. Primary staining was performed with monoclonal antibodies against the phosphorylated proteins, rabbit anti-p-ERK (1:200; cat. no. 4370S, Cell Signaling Technology), rabbit anti-p-Akt (1:100; cat. no. 2965S, Cell Signaling Technology), rabbit anti-p-STAT3 (1:100; cat. no. 9145S, Cell Signaling Technology), mouse anti-p-JNK (1:200; cat. no. 9255S, Cell Signaling Technology) and anti-p-p38 (cat. no. 4511S 1:800; Cell Signaling

Technology) followed by addition of secondary Alexa-Fluor-488-conjugated antibodies (1:1000; Life Technologies). The measurements were performed on an Attune Flow Cytometer (Life Technologies) and analyzed with Flowjo V10 software (Flowjo, Ashland, OR).

### BrdU incorporation assay for cell cycle and proliferation analysis

Cell proliferation and cell cycle were measured following incubation in culture for 30 min or 2 h with 0.2 mM BrdU (Sigma-Aldrich) (Cappella et al., 2008; Oliveira et al., 2013). Cells were fixed with ice-cold ethanol for at least 4 h, incubated in 1.5 M HCl for 30 min and 0.1 M borate buffer (pH 8.0) for 5 min. Cells were then incubated with antibodies rat anti-BrdU (1:200; cat. no. OBT0030, Accurate Chemical) or rabbit anti-Ki67 (1:500; cat. no. AB9260, Chemicon-Millipore) antibodies. Some samples (depending on the analysis) were incubated with propidium iodide (50 µg/ml; Life Techologies) and RNAse A (50 µg/ml; Life Techologies) for 20 min. Flow cytometry events were gated by FL2A versus FL2H for doublet exclusion.

To better characterize the influence of bradykinin on proliferation, the duration of cell cycle and its phases were examined by two methods with flow cytometry experiments. With the first analysis (A), according to Nowakowski et al. (1989) and Lukaszewicz et al. (2002), it is possible to calculate the duration of the cell cycle, S-phase and the combined duration of $G_1$, $G_2$ and M phases ($G_1$+$G_2$/M). These parameters were determined by computing the labeling index values (BrdU treatment for 30 min and 2 h) within the population of cycling cells ($Ki67^+$; proliferation fraction). In the second analysis (B), adapted from immunohistochemistry experiments of Storey et al. (1989) and Wilcock et al. (2007), simultaneous equations were used to calculate the duration of the cell cycle and S-phase. That is, (1) length of S phase (denoted Ts)+[30 min (of treatment)−6 min]=percentage of S-phase cells labeled in pulse×total time of cell cycle (denoted Tc) and (2) Ts+(120 min−6 min)=percentage of S-phase cells labeled in pulse×Tc. Furthermore, the length of the $G_2$/M phase=percentage of cells in $G_2$/M phase (revealed by propidium iodide staining)×Tc. Finally, length of $G_1$ phase=Tc–Ts–time in G2 and M (denoted $TG_2$/M) or length of $G_1$ phase=time in $G_1$, $G_2$ and M phases (denoted $TG_1$+$G_2$/M)–$TG_2$/M. A minimum of 60,000 cells were analyzed per sample.

### Extraction of nuclear and cytosolic fractions and western blotting assays

Separation of nuclear and cytosolic fractions was performed with the NE-PER® Nuclear and Cytoplasmic Extraction Reagents kit (Thermo Scientific, Waltham, MA). Protein in sample buffer was separated by SDS-PAGE on a 10% polyacrylamide gel. Proteins were then transferred to a nitrocellulose membrane (Thermo Scientific) in a wet system for 1 h at constant amperage of 400 mA. The membranes were incubated with primary antibodies, such as rabbit anti-p-ERK1/2 (1:1000, cat. no. 9101, Cell Signaling Technology), mouse anti-ERK1/2 (1:1000, cat. no. SC-514302, Santa Cruz Biotechnology, Dallas, TX), goat anti-Histone H1 (1:1000, sc 34464, Santa Cruz Biotechnology) and mouse anti-β-actin (1:1000, cat. no. A5441, Sigma-Aldrich) plus 1% BSA in Tris-buffered saline with 0.03% Tween-20 (TBS-T) overnight at 4°C. Membranes were probed with the respective secondary antibodies for 1 h under agitation at room temperature. Membranes were scanned with a laser scanner for biomolecular imaging applications (Typhoon™, GE Healthcare). Detected bands were submitted to densitometric analysis with the ImageJ software (National Institutes of Health; this software can be obtained from http://imagej.net/Welcome).

### Reverse transcription and quantitative polymerase chain reaction

Total RNA was obtained using the Trizol reagent (Life Technologies). After DNAse I treatment, cDNAs were produced by SuperScript II Reverse Transcriptase (Life Technologies). Specific mRNAs were analyzed by SYBR Green real-time PCR on the ABI StepOnePlus Instrument (Life Technologies). Primer sequences were: *Hes1*, forward primer 5′-TGCCTTTCTCATCCCCAACG-3′ and reverse primer 5′-AGGTGACACTGCGTTAGGAC-3′; *GAPDH*, forward primer 5′-TGCACCACCAACTGCTTAG-3′ and reverse primer 5′-GGATGCAGGGATGATGTTC-3′; *TIS21*, forward primer 5′-ATGAGCCACGGGAAGAGAAC-3′ and reverse primer 5′-GCCCTACTGAAAACCTTGAGTC-3′; *Mash1*, forward primer 5′-GCCTCCAATTGAAGCAACGTC-3′ and reverse primer 5′-AGAAGCAAAGACCGTGGGAG-3′; *Ngn2*, forward primer 5′-TCGGCTTTAACTGGAGTGCC-3′ and reverse primer 5′-GTGTGTTGTCGTTCTCGTGC-3′. Thermal cycling conditions consisted of 50°C for 2 min, 95°C for 10 min, and 50 cycles of 95°C for 15 s and 60°C for 1 min. The $2^{-\Delta\Delta Ct}$ parameter was used for quantification and *GAPDH* gene expression was used as internal standard (Lameu et al., 2012; Livak and Schmittgen, 2001).

### Statistical analysis

The results are expressed as mean±s.e.m. from three or more independent experiments. Statistical comparisons between different treatments, with normal distribution, were performed by either a Student's *t*-test and/or two-way analysis of variance (ANOVA) with a Bonferroni post hoc test by using GraphPad Prism 5.1 software (La Jolla, CA). The criteria for statistical significance were set at $P<0.05$. For flow cytometry, a minimum of 30,000 cells was analyzed per sample. A minimum of 300 and up to 800 cells per sample was counted for quantification of immunolabeled cells or cells captured by differential interference contrast (DIC) microscopy.

#### Acknowledgements

We thank Dr Rupert Ecker (TissueGnostics GMBH, Vienna, Austria) for automatic analysis of hippocampal slices for Ki67 expression.

#### Competing interests

The authors declare no competing or financial interests.

#### Author contributions

M.M.P., C.L., C.A.T., T.G., P.D.N. and A.R.C. performed the research. M.M.P., H.U., A.M.O.B., T.T.S., A.M.O.B. and A.R.M. helped in the design and data interpretation. H.U. supervised the study. H.U., A.M.O.B. and A.R.M. obtained financing for the study. M.M.P. and H.U. prepared the manuscript.

#### Funding

This work was supported by research grants and fellowships from Fundação de Amparo à Pesquisa do Estado de São Paulo (FAPESP) [grant number 2012/50880-4]; Conselho Nacional de Desenvolvimento Científico e Tecnológico, Brazil (CNPq) [grant number 467465/2014-2]; the California Institute for Regenerative Medicine (CIRM) [grant numbers TR4-06747, DISC-08825]; the National Institutes of Health through the NIH Director's New Innovator Award Program [grant numbers 1-DP2-OD006495-01, R01MH103134, R01MH094753, R21MH107771] and a NARSAD Independent Investigator Grant to A.R.M. M.M.P and T.G. are grateful for post-doctoral fellowships from FAPESP. Deposited in PMC for release after 12 months.

#### Supplementary information

Supplementary information available online at
http://jcs.biologists.org/lookup/doi/10.1242/jcs.192534.supplemental

#### References

**Appell, K. C. and Barefoot, D. S.** (1989). Neurotransmitter release from bradykinin-stimulated PC12 cells. Stimulation of cytosolic calcium and neurotransmitter release. *Biochem. J.* **263**, 11-18.

**Blaukat, A., Barac, A., Cross, M. J., Offermanns, S. and Dikic, I.** (2000). G protein-coupled receptor-mediated mitogen-activated protein kinase activation through cooperation of Galpha(q) and Galpha(i) signals. *Mol. Cell. Biol.* **20**, 6837-6848.

**Bouschet, T., Perez, V., Fernandez, C., Bockaert, J., Eychene, A. and Journot, L.** (2003). Stimulation of the ERK pathway by GTP-loaded Rap1 requires the concomitant activation of Ras, protein kinase C, and protein kinase A in neuronal cells. *J. Biol. Chem.* **278**, 4778-4785.

**Calegari, F. and Huttner, W. B.** (2003). An inhibition of cyclin-dependent kinases that lengthens, but does not arrest, neuroepithelial cell cycle induces premature neurogenesis. *J. Cell Sci.* **116**, 4947-4955.

**Calegari, F., Haubensak, W., Haffner, C. and Huttner, W. B.** (2005). Selective lengthening of the cell cycle in the neurogenic subpopulation of neural progenitor cells during mouse brain development. *J. Neurosci.* **25**, 6533-6538.

**Cappella, P., Gasparri, F., Pulici, M. and Moll, J.** (2008). A novel method based on click chemistry, which overcomes limitations of cell cycle analysis by classical determination of BrdU incorporation, allowing multiplex antibody staining. *Cytometry A* **73A**, 626-636.

**Chen, J., DeVivo, M., Dingus, J., Harry, A., Li, J., Sui, J., Carty, D. J., Blank, J. L., Exton, J. H., Stoffel, R. H. et al.** (1995). A region of adenylyl cyclase 2 critical for regulation by G protein beta gamma subunits. *Science* **268**, 1166-1169.

**Chow, S., Patel, H. and Hedley, D. W.** (2001). Measurement of MAP kinase activation by flow cytometry using phospho-specific antibodies to MEK and ERK: potential for pharmacodynamic monitoring of signal transduction inhibitors. *Cytometry* **46**, 72-78.

**Dixon, B. S., Evanoff, D., Fang, W. B. and Dennis, M. J.** (2002). Bradykinin B1 receptor blocks PDGF-induced mitogenesis by prolonging ERK activation and increasing p27Kip1. *Am. J. Physiol. Cell Physiol.* **283**, C193-C203.

**Duchene, J., Schanstra, J. P., Pecher, C., Pizard, A., Susini, C., Esteve, J.-P., Bascands, J.-L. and Girolami, J.-P.** (2002). A novel protein-protein interaction between a G protein-coupled receptor and the phosphatase SHP-2 is involved in bradykinin-induced inhibition of cell proliferation. *J. Biol. Chem.* **277**, 40375-40383.

**Ebisuya, M., Kondoh, K. and Nishida, E.** (2005). The duration, magnitude and compartmentalization of ERK MAP kinase activity: mechanisms for providing signaling specificity. *J. Cell Sci.* **118**, 2997-3002.

**Hall, J. M., Caulfield, M. P., Watson, S. P. and Guard, S.** (1993). Receptor subtypes or species homologues: relevance to drug discovery. *Trends Pharmacol. Sci.* **14**, 376-383.

**Hanke, S., Valkova, C., Stirnweiss, J., Drube, S. and Liebmann, C.** (2006). Activated EGF receptor may balance ERK-inhibitory network signalling pathways. *Cell Signal.* **18**, 1031-1040.

**Iacopetti, P., Michelini, M., Stuckmann, I., Oback, B., Aaku-Saraste, E. and Huttner, W. B.** (1999). Expression of the antiproliferative gene TIS21 at the onset of neurogenesis identifies single neuroepithelial cells that switch from proliferative to neuron-generating division. *Proc. Natl. Acad. Sci. USA* **96**, 4639-4644.

**Imayoshi, I., Shimogori, T., Ohtsuka, T. and Kageyama, R.** (2008). Hes genes and neurogenin regulate non-neural versus neural fate specification in the dorsal telencephalic midline. *Development* **135**, 2531-2541.

**Impey, S., Obrietan, K. and Storm, D. R.** (1999). Making new connections: role of ERK/MAP kinase signaling in neuronal plasticity. *Neuron* **23**, 11-14.

**Kageyama, R., Ohtsuka, T., Shimojo, H. and Imayoshi, I.** (2008). Dynamic Notch signaling in neural progenitor cells and a revised view of lateral inhibition. *Nat. Neurosci.* **11**, 1247-1251.

**Khoury, E., Nikolajev, L., Simaan, M., Namkung, Y. and Laporte, S. A.** (2014). Differential regulation of endosomal GPCR/beta-arrestin complexes and trafficking by MAPK. *J. Biol. Chem.* **289**, 23302-23317.

**Krutzik, P. O. and Nolan, G. P.** (2003). Intracellular phospho-protein staining techniques for flow cytometry: monitoring single cell signaling events. *Cytometry A* **55A**, 61-70.

**Lako, M., Neganova, I. and Armstrong, L.** (2009). G1 to S transition and pluripotency: two sides of the same coin? *Cell Cycle* **8**, 1105-1111.

**Lamb, M. E., De Weerd, W. F. C. and Leeb-Lundberg, L. M. F.** (2001). Agonist-promoted trafficking of human bradykinin receptors: arrestin- and dynamin-independent sequestration of the B2 receptor and bradykinin in HEK293 cells. *Biochem. J.* **355**, 741-750.

**Lameu, C., Trujillo, C. A., Schwindt, T. T., Negraes, P. D., Pillat, M. M., Morais, K. L., Lebrun, I. and Ulrich, H.** (2012). Interactions between the NO-citrulline cycle and brain-derived neurotrophic factor in differentiation of neural stem cells. *J. Biol. Chem.* **287**, 29690-29701.

**Liebmann, C., Offermanns, S., Spicher, K., Hinsch, K.-D., Schnittler, M., Morgat, J. L., Reissmann, S., Schultz, G. and Rosenthal, W.** (1990). A high-affinity bradykinin receptor in membranes from rat myometrium is coupled to pertussis toxin-sensitive G-proteins of the Gi family. *Biochem. Biophys. Res. Commun.* **167**, 910-917.

**Liebmann, C., Graness, A., Ludwig, B., Adomeit, A., Boehmer, A., Boehmer, F. D., Nürnberg, B. and Wetzker, R.** (1996). Dual bradykinin B2 receptor signalling in A431 human epidermoid carcinoma cells: activation of protein kinase C is counteracted by a GS-mediated stimulation of the cyclic AMP pathway. *Biochem. J.* **313**, 109-118.

**Livak, K. J. and Schmittgen, T. D.** (2001). Analysis of relative gene expression data using real-time quantitative PCR and the 2(-Delta Delta C(T)) Method. *Methods* **25**, 402-408.

**Lukaszewicz, A., Savatier, P., Cortay, V., Kennedy, H. and Dehay, C.** (2002). Contrasting effects of basic fibroblast growth factor and neurotrophin 3 on cell cycle kinetics of mouse cortical stem cells. *J. Neurosci.* **22**, 6610-6622.

**Marshall, C. J.** (1995). Specificity of receptor tyrosine kinase signaling: transient versus sustained extracellular signal-regulated kinase activation. *Cell* **80**, 179-185.

**Martins, A. H. B., Resende, R. R., Majumder, P., Faria, M., Casarini, D. E., Tarnok, A., Colli, W., Pesquero, J. B. and Ulrich, H.** (2005). Neuronal differentiation of P19 embryonal carcinoma cells modulates kinin B2 receptor gene expression and function. *J. Biol. Chem.* **280**, 19576-19586.

**Martins, A. H., Alves, J. M., Trujillo, C. A., Schwindt, T. T., Barnabé, G. F., Motta, F. L. T., Guimaraes, A. O., Casarini, D. E., Mello, L. E., Pesquero, J. B. et al.** (2008). Kinin-B2 receptor expression and activity during differentiation of embryonic rat neurospheres. *Cytometry A* **73A**, 361-368.

**Munoz, C. M., Cotecchia, S. and Leeb-Lundberg, L. M.** (1993). B2 kinin receptor-mediated internalization of bradykinin in DDT1 MF-2 smooth muscle cells is paralleled by sequestration of the occupied receptors. *Arch. Biochem. Biophys.* **301**, 336-344.

**Murray, A. W.** (1998). MAP kinases in meiosis. *Cell* **92**, 157-159.

**Nakamura, Y., Sakakibara, S., Miyata, T., Ogawa, M., Shimazaki, T., Weiss, S., Kageyama, R. and Okano, H.** (2000). The bHLH gene hes1 as a repressor of the neuronal commitment of CNS stem cells. *J. Neurosci.* **20**, 283-293.

**Nascimento, I. C., Glaser, T., Nery, A. A., Pillat, M. M., Pesquero, J. B. and Ulrich, H.** (2015). Kinin-B1 and B2 receptor activity in proliferation and neural phenotype determination of mouse embryonic stem cells. *Cytometry A* **87**, 989-1000.

**Neganova, I., Zhang, X., Atkinson, S. and Lako, M.** (2009). Expression and functional analysis of G1 to S regulatory components reveals an important role for CDK2 in cell cycle regulation in human embryonic stem cells. *Oncogene* **28**, 20-30.

**Nowakowski, R. S., Lewin, S. B. and Miller, M. W.** (1989). Bromodeoxyuridine immunohistochemical determination of the lengths of the cell cycle and the DNA-synthetic phase for an anatomically defined population. *J. Neurocytol.* **18**, 311-318.

**Oliveira, S. L. B., Pillat, M. M., Cheffer, A., Lameu, C., Schwindt, T. T. and Ulrich, H.** (2013). Functions of neurotrophins and growth factors in neurogenesis and brain repair. *Cytometry A* **83**, 76-89.

**Orford, K. W. and Scadden, D. T.** (2008). Deconstructing stem cell self-renewal: genetic insights into cell-cycle regulation. *Nat. Rev. Genet.* **9**, 115-128.

**Pillat, M. M., Cheffer, A., de Andrade, C. M., Morsch, V. M., Schetinger, M. R. C. and Ulrich, H.** (2015). Bradykinin-induced inhibition of proliferation rate during neurosphere differentiation: consequence or cause of neuronal enrichment? *Cytometry A* **87**, 929-935.

**Reffas, S. and Schlegel, W.** (2000). Compartment-specific regulation of extracellular signal-regulated kinase (ERK) and c-Jun N-terminal kinase (JNK) mitogen-activated protein kinases (MAPKs) by ERK-dependent and non-ERK-dependent inductions of MAPK phosphatase (MKP)-3 and MKP-1 in differentiating P19 cells. *Biochem. J.* **352**, 701-708.

**Reynolds, B. A. and Weiss, S.** (1992). Generation of neurons and astrocytes from isolated cells of the adult mammalian central nervous system. *Science* **255**, 1707-1710.

**Reynolds, B. A. and Weiss, S.** (1996). Clonal and population analyses demonstrate that an EGF-responsive mammalian embryonic CNS precursor is a stem cell. *Dev. Biol.* **175**, 1-13.

**Santos, S. D. M., Verveer, P. J. and Bastiaens, P. I. H.** (2007). Growth factor-induced MAPK network topology shapes Erk response determining PC-12 cell fate. *Nat. Cell Biol.* **9**, 324-330.

**Sasagawa, S., Ozaki, Y.-i., Fujita, K. and Kuroda, S.** (2005). Prediction and validation of the distinct dynamics of transient and sustained ERK activation. *Nat. Cell Biol.* **7**, 365-373.

**Shah, B. H., Siddiqui, A., Qureshi, K. A., Khan, M., Rafi, S., Ujan, V. A., Yaqub, M. Y., Rasheed, H. and Saeed, S. A.** (1999). Co-activation of Gi and Gq proteins exerts synergistic effect on human platelet aggregation through activation of phospholipase C and Ca2+ signalling pathways. *Exp. Mol. Med.* **31**, 42-46.

**Storey, K. G.** (1989). Cell lineage and pattern formation in the earthworm embryo. *Development* **107**, 519-531.

**Tischler, A. S. and Greene, L. A.** (1975). Nerve growth factor-induced process formation by cultured rat pheochromocytoma cells. *Nature* **258**, 341-342.

**Traverse, S., Gomez, N., Paterson, H., Marshall, C. and Cohen, P.** (1992). Sustained activation of the mitogen-activated protein (MAP) kinase cascade may be required for differentiation of PC12 cells. Comparison of the effects of nerve growth factor and epidermal growth factor. *Biochem. J.* **288**, 351-355.

**Tropepe, V., Sibilia, M., Ciruna, B. G., Rossant, J., Wagner, E. F. and van der Kooy, D.** (1999). Distinct neural stem cells proliferate in response to EGF and FGF in the developing mouse telencephalon. *Dev. Biol.* **208**, 166-188.

**Trujillo, C. A., Schwindt, T. T., Martins, A. H., Alves, J. M., Mello, L. E. and Ulrich, H.** (2009). Novel perspectives of neural stem cell differentiation: from neurotransmitters to therapeutics. *Cytometry A* **75A**, 38-53.

**Trujillo, C. A., Negraes, P. D., Schwindt, T. T., Lameu, C., Carromeu, C., Muotri, A. R., Pesquero, J. B., Cerqueira, D. M., Pillat, M. M., de Souza, H. D. et al.** (2012). Kinin-B2 receptor activity determines the differentiation fate of neural stem cells. *J. Biol. Chem.* **287**, 44046-44061.

**Vaudry, D., Stork, P. J. S., Lazarovici, P. and Eiden, L. E.** (2002). Signaling pathways for PC12 cell differentiation: making the right connections. *Science* **296**, 1648-1649.

**von Kriegsheim, A., Baiocchi, D., Birtwistle, M., Sumpton, D., Bienvenut, W., Morrice, N., Yamada, K., Lamond, A., Kalna, G., Orton, R. et al.** (2009). Cell fate decisions are specified by the dynamic ERK interactome. *Nat. Cell Biol.* **11**, 1458-1464.

**Westermarck, J., Li, S.-P., Kallunki, T., Han, J. and Kahari, V.-M.** (2001). p38 mitogen-activated protein kinase-dependent activation of protein phosphatases 1 and 2A inhibits MEK1 and MEK2 activity and collagenase 1 (MMP-1) gene expression. *Mol. Cell. Biol.* **21**, 2373-2383.

**Wilcock, A. C., Swedlow, J. R. and Storey, K. G.** (2007). Mitotic spindle orientation distinguishes stem cell and terminal modes of neuron production in the early spinal cord. *Development* **134**, 1943-1954.

**York, R. D., Yao, H., Dillon, T., Ellig, C. L., Eckert, S. P., McCleskey, E. W. and Stork, P. J.** (1998). Rap1 mediates sustained MAP kinase activation induced by nerve growth factor. *Nature* **392**, 622-626.